Int. J. Solids Structures Vol. 21, No. 2, pp. 161–176, 1985
Printed in the U.S.A.

0020-7683/85 $3.00 + .00

SMOOTH INDENTATION OF AN INITIALLY STRESSED ORTHOTROPIC BEAM

C. T. SUN AND B. V. SANKAR
School of Aeronautics and Astronautics, Purdue University, West Lafayette, IN 47907, U.S.A.

(*Received* 29 *July* 1983; *in revised form* 23 *April* 1984)

Abstract—The contact behavior between a smooth rigid cylinder and a simply supported orthotropic beam under uniaxial initial stresses is studied. The displacements are computed by superposing Mindlin plate solution with the solution obtained from Biot's theory of incremental deformation. Finite Fourier transforms are used in solving the equations. A point matching technique is used to compute the contact stresses and the amount of indentation for a given contact length. The effects of orthotropy and initial stresses on the contact stress distribution are investigated. An indentation law is established from the numerical results.

NOTATION

a_n	Fourier coefficients
$b_1, \ldots, b_4, d_1, \ldots, d_4$	elasticity solution constants
B_{ij}	incremental stiffness coefficients
c	semi contact length
C_{ij}	elastic constants of the orthotropic medium
E_1, E_3	Young's moduli
G_{13}	Shear modulus
h	beam thickness
i	square root of -1
k	transverse shear correction factor
k^*	dimensionless contact coefficient
L	half length of beam
n	transform variable
N_x^0	initial stress resultant
$p(x)$	load distribution
P	total load
q	exponent in indentation law
q_j	magnitude of jth pressure distribution
R	radius of indenter
S_0	magnitude of initial stress in the x-direction
s_{ij}	incremental stress components in Biot's theory
u	horizontal displacement
w	vertical displacement
w_0	vertical displacement at the center
w_{jk}	vertical displacement of jth point due to kth load distribution of unit magnitude
x, z	horizontal and vertical coordinate axes
α	indentation
γ_{ij}	incremental shear strain
ϵ_x, ϵ_z	incremental normal strains
Θ	slope of deflection curve at the supports (calculated from beam theory)
λ_1, λ_3	principal elongations due to initial stresses
ν_{13}, ν_{31}	Poisson's ratios
ξ	transform variable ($= n\pi/L$)
$\rho_1, \ldots, \rho_4$	roots of the characteristic equation
σ_x, σ_z	incremental normal stresses
τ_{xz}	incremental shear stress
ψ	beam rotation in the xz plane
ω	local rotation of a material element

1. INTRODUCTION

The problem of smooth indentation of an isotropic beam by a rigid cylinder was studied by Keer and Miller [1]. Their method superposes an infinite layer solution derived through the use of integral transforms with a pure bending beam theory solution. The problem is reduced to a Fredholm integral equation of second kind, which is solved numerically. Keer and Ballarini [2] used a similar method as above to solve the problem of contact between a rigid indenter and an initially stressed orthotropic beam. The

elasticity solution for transverse loading on an initially stressed, infinitely long layer was obtained using an exact rate formulation in terms of the first Piola-Kirchhoff stress components referred to the current configuration. They derived expressions for contact stresses and beam compliances for various combinations of initial stresses and boundary conditions.

Sankar and Sun [3] approached the same problem in a simpler way. They first considered the two-dimensional problem of a beam subjected to an arbitrary but symmetrical loading. The loading was considered as the sum of an uniformly distributed load (U.D.L.) and a varying part of zero average value. The deflection due to U.D.L. was obtained from the classical beam theory. The displacements due to the varying part of the load were evaluated by solving the plane elasticity equations using finite Fourier transforms. The problem of indentation was solved by using the above procedures in conjunction with a point matching technique.

In this paper, a similar approach is used to solve the problem of indentation of an orthotropic beam by a rigid cylinder. The cases wherein the beam is under initial stresses along the longitudinal direction are also considered. The indenter is assumed to be smooth, i.e. there is no friction under the indenter. Section 2 deals with a method to solve the two-dimensional problem of an orthotropic beam subjected to uniform initial stresses along the longitudinal direction and an arbitrary symmetrical transverse loading on one side of the beam. The transverse loading is considered as the superposition of an U.D.L. and a varying part of zero average value. The deflection of the beam due to U.D.L. is obtained by using Mindlin plate theory which accounts for shear deformation. The effect of the axial force is also included in the above formulation. The displacements due to the varying part of the transverse loading are evaluated by solving the plane elasticity equations using finite Fourier transforms. Biot's theory of incremental deformations is used to formulate the equations of equilibrium when the beam is subjected to initial stresses. The above mentioned theory has been discussed in detail in [4]. Essentially, Biot's method involves separating the rotations from pure deformations. This is achieved by referring the stresses and strains to coordinate systems which rotate with the material elements at each point. Then it is argued that the incremental stresses depend linearly on the incremental strains referred to the rotated coordinates. The equilibrium equations in displacements u and w, after linearization, look similar to the conventional equations except for that the elastic constants appear to have been modified by the presence of initial stresses.

The problem of indentation is discussed in Section 3. The contact length is assumed to be known *a priori* and the contact stresses are computed using a point matching technique. It has been found that for small contact lengths, the contact stress distribution is elliptical and this fact is used to solve the problem in a direct way. The above method is referred to as the method of assumed stress distribution.

Numerical examples and discussions are presented in Section 4. In the examples, the orthotropic medium is assumed to be a fiber-reinforced composite and the properties are computed using the rule of mixtures. The elastic constants of the fiber and matrix materials and the volume ratios are assumed suitably. The quantities of interest in such problems are: variation of contact length with the load, contact stress distribution, overall beam stiffness and load-indentation relationship. Indentation is defined as the difference in the displacement of the indenter and that of the corresponding point on the bottom surface of the beam. Our discussions are focussed on two aspects, namely, the effect of anisotropy of the beam material and the effect of initial stresses in the beam.

The results of such static contact problems are very useful in the study of transverse impact problems. For example, Sun and Chattopadhyay [5] used a Hertzian type contact law to compute the impact force history. The increasing use of composite materials in aerospace as well as automobile structures has generated a great interest in the low velocity impact problems. The formulation of such problems are based on the assumption that the elastodynamic effects occur during a short interval of time, and hence the local deformation and stresses can be approximated by the elastostatic solution for

indentation. Moreover, an impacted structure may be under a state of initial stresses during foreign object impact, e.g. composite facing of a sandwich beam under bending loads, jet engine fan blades subjected to centrifugal forces. In such situations the methods of analysis presented here will be very useful. It is shown that the Young's modulus in the transverse direction and also the initial stresses in the beam can significantly alter the local contact behavior.

2. AUXILIARY PROBLEM

The problem to be discussed in this section is depicted in Fig. 1. The beam material is assumed to be orthotropic with the material axes of symmetry parallel to the coordinate axes. The width of the beam (in the y-direction) is assumed to be unity. Uniform initial stresses of magnitude S_0 are assumed to be present in the x-direction. Also, the beam is supposed to be simply supported. The case of clamped ends can be treated in an analogous manner. The load $p(x)$ is arbitrary, but assumed to be symmetrical about the center of the beam. The function $p(x)$ can be expressed in the form of a complex Fourier series in the interval $-L$ to $+L$. Thus,

$$p(x) = \frac{P}{2L} + \sum_{\substack{n=-\infty \\ n\neq 0}}^{\infty} a_n e^{in\pi x/L} \tag{1}$$

where P is the total load given by

$$P = \int_{-c}^{+c} p(x)\,dx$$

and a_n are the Fourier coefficients expressed by the formula

$$a_n = \frac{1}{2L}\int_{-L}^{+L} p(x)e^{-in\pi x/L}\,dx. \tag{2}$$

Actually, the load $p(x)$ can be considered as the sum of two types of loadings, namely, an U.D.L. of intensity $P/2L$ and a varying part $p_1(x)$. Thus eqn (1) may be written as

$$p(x) = \frac{p}{2L} + p_1(x). \tag{3}$$

The methods of finding the displacements due to each part of the applied load are discussed below.

2.1. *Deflection due to* U.D.L.

We assume a state of plane-strain parallel to the x-z plane. The constitutive relations

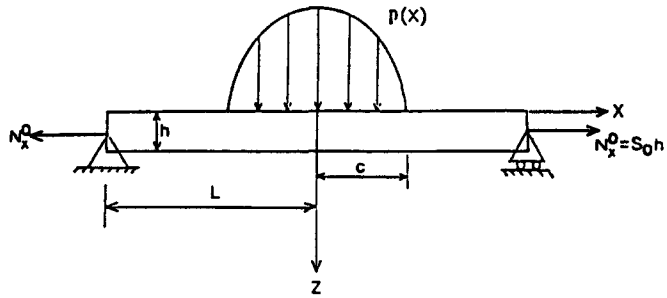

Fig. 1. Orthotropic beam subjected to axial initial stresses and an arbitrary, symmetrical transverse loading.

of the orthotropic medium are given by

$$\begin{bmatrix} \sigma_x \\ \sigma_z \\ \tau_{xz} \end{bmatrix} = \begin{bmatrix} C_{11} & C_{13} & 0 \\ C_{13} & C_{33} & 0 \\ 0 & 0 & C_{55} \end{bmatrix} \begin{bmatrix} \epsilon_x \\ \epsilon_z \\ \gamma_{xz} \end{bmatrix} \tag{4}$$

where σ_x, σ_z, τ_{xz} and ϵ_x, ϵ_z and γ_{xz} are incremental stresses and strains due to the transverse loading and they are referred to x and z axes. The elastic constants C_{ij} are assumed to be the same as those in the natural state. This assumption is reasonable for solids which do not experience large deformations and rotations when subjected to the initial stresses. These constants can be related to the orthotropic engineering elastic constants E_1, E_2, etc.

We shall use the plate bending equations developed by Whitney and Pagano [6]. The initial stresses along the x-axis are accounted by adding the term $N_x^0 w_{,xx}$ to the loading term $P/2L$. Thus the equations of equilibrium are [5]:

$$D_{11}\psi_{,xx} - kA_{55}(\psi + w_{,x}) = 0 \tag{5}$$

$$kA_{55}(\psi_{,x} + w_{,xx}) + \left(\frac{P}{2L} + N_x^0 w_{,xx}\right) = 0 \tag{6}$$

In the above equations, N_x^0 is the initial stress resultant, $w(x)$ is the transverse displacement, ψ is the rotation about y-axis, k, the transverse shear correction factor is taken to be 0.67 and

$$D_{11} = Q_{11}h^3/12, \quad Q_{11} = C_{11} - C_{13}^2/C_{33}, \quad A_{55} = C_{55}h.$$

Equations (5–6) are ordinary simultaneous differential equations in variables $\psi(x)$ and $w(x)$ which may be solved using Fourier transforms. The following boundary conditions have to be used to solve for the arbitrary constants involved in the solution. The boundary conditions are: at $x = \pm L$, $\psi_{,x} = 0$ and $w = 0$. The final solution for the transverse displacement is given by

$$w(x') = (PD_{11}/2LN_x^{0^2})(-1 + \cosh\sqrt{\beta N_x^0}x' - \tanh\sqrt{\beta N_x^0}L \sinh\sqrt{\beta N_x^0}x') + \frac{Px'}{2N_x^0} - \frac{Px'^2}{4LN_x^0} \tag{7}$$

where

$$x' = x + L, \quad \beta = kA_{55}/D_{11}(N_x^0 + kA_{55}).$$

2.2. *Displacements due to $p_1(x)$*

In this section we describe the method of solving the two dimensional problem of an orthotropic beam under initial stresses, subjected to transverse loading $p_1(x)$. As mentioned earlier, the approach we are going to use is that of Biot, which has been discussed in detail in [4]. The assumptions used in the present analysis are as follows. Plane strain condition is assumed along the y-direction, i.e. $\epsilon_{yy} = \gamma_{yx} = \gamma_{yz} = 0$. The initial stresses do not change the planes of material symmetry of the original orthotropic medium. So, the incremental stress-strain relations are also orthotropic. The relevant equilibrium equations are [4]:

$$\begin{aligned} s_{11,x} + s_{13,z} + S_0\omega_{,z} &= 0 \\ s_{13,x} + s_{33,z} + S_0\omega_{,x} &= 0 \end{aligned} \tag{8}$$

where S_0 is the initial stress along the x-direction, s_{11}, s_{33} and x_{13} are incremental

stresses referred to axes 1, 3 which rotate locally with the material. The local rotation ω is given by

$$\omega = \tfrac{1}{2}(w_{,x} - u_{,z})$$

where $u(x, z)$ denotes the horizontal displacement. The incremental strains for small incremental deformations are given by

$$\epsilon_x = u_{,x}, \quad \epsilon_z = w_{,z}, \quad \gamma_{xz} = w_{,x} + u_{,z}. \tag{9}$$

Biot's theory assumes that incremental stress-strain relations are linear as given below:

$$\begin{bmatrix} s_{11} \\ s_{33} \\ s_{13} \end{bmatrix} = \begin{bmatrix} B_{11} & b_{13} & 0 \\ B_{31} & b_{33} & 0 \\ 0 & 0 & Q_3 \end{bmatrix} \begin{bmatrix} \epsilon_x \\ \epsilon_z \\ \gamma_{xz} \end{bmatrix}. \tag{10}$$

The stiffness coefficients B_{ij} are generally functions of the elastic constants of the original orthotropic medium and the initial stress S_0. The details of derivation of these coefficients are given in [4] and only the results are presented here.

Let λ_1 and λ_3 be the principal elongations in directions x and z due to the initial stress S_0. Physically this means that an unit square in the x-z plane deforms into a rectangle of dimensions λ_1 and λ_3 due to application of initial stresses. We assume that the material is linearly elastic and use the constitutive relations (4) to compute λ_1 and λ_3. The incremental elastic coefficients B_{ij} are expressed in terms of the elastic coefficients of the original orthotropic medium and the principal elongations λ_1 and λ_2 as

$$\begin{aligned} B_{11} &= \lambda_1 C_{11} \\ B_{33} &= \lambda_3 C_{33} \\ B_{31} &= S_0 + \lambda_3 C_{13} \\ B_{13} &= \lambda_3 C_{13} \\ Q_3 &= C_{55}(\lambda_1 + \lambda_3)/2. \end{aligned} \tag{11}$$

It may be noted that B_{13} is not equal to B_{31}. This is because of lack of symmetry in the initial stress state.

Using the incremental stress-strain relations (10) and the strain-displacement relations (9), equilibrium equations (8) can be reduced to the following form:

$$\begin{aligned} A_1 u_{,xx} + A_2 u_{,zz} + A_3 w_{,xz} &= 0 \\ A_4 w_{,zz} + A_5 w_{,xx} + A_3 u_{,xz} &= 0 \end{aligned} \tag{12}$$

where

$$\begin{aligned} A_1 &= B_{11} \\ A_2 &= Q_3 - S_0/2 \\ A_3 &= B_{31} + Q_3 - S_0/2 \\ A_4 &= B_{33} \\ A_5 &= Q_3 + S_0/2. \end{aligned}$$

One can note that the equations of equilibrium (12) are similar to those for an orthotropic medium without initial stresses, except that the elastic constants are modified by the presence of initial stresses.

In the case of initial stress problems, the stress boundary conditions are called "incremental boundary force conditions" [4]. The incremental boundary forces Δf_x and Δf_z can be expressed in terms of the incremental stresses s_{11}, s_{13}, s_{33} and the initial stress S_0. For the problem in consideration, the incremental boundary force conditions are as follows:

$$\begin{aligned} \text{on } z = h,\ \Delta f_x &= (s_{13} - S_0\gamma_{xz}/2) = 0 \\ \Delta f_z &= s_{33} = 0 \\ \text{on } z = 0,\ \Delta f_x &= (s_{13} - S_0\gamma_{xz}/2) = 0 \\ \Delta f_z &= -s_{33} = p_1(x). \end{aligned} \tag{13}$$

We use finite Fourier transforms to solve the set of partial differential equations (12). The Fourier transform of $f(x)$ is defined as

$$f(n) = \frac{1}{2L}\int_{-L}^{+L} f(x)e^{-in\pi x/L}\,dx.$$

Then the inverse transform is

$$f(x) = f_0 + \sum_{\substack{n=-\infty \\ n\neq 0}}^{+\infty} \bar{f}(n)e^{in\pi x/L} \tag{14}$$

where f_0 is the average value of the function over the interval $-L$ to $+L$. From eqns (1–3) we obtain

$$\begin{aligned} \bar{p}_1(n) &= a_n; \quad n \neq 0 \\ &= 0; \quad n = 0. \end{aligned} \tag{15}$$

Taking Fourier transforms of both sides of eqn (12), we have to transform functions such as $u_{,xx}$ and impose certain displacement boundary conditions. We shall use the following approximations in addition to the known condition $w(\pm L, z) = 0$. First, we assume that

$$w_{,x}(\mp L, z) = \pm\Theta$$

where Θ is the average slope at the ends of the beam due to load $p_1(x)$ evaluated using Mindlin plate theory. The axial force in the beam should also be taken into consideration. In addition, we assume that plane sections remain plane after bending, which leads to the boundary condition

$$u(\pm L, z) = \pm\left(z - \frac{h}{2}\right)\Theta.$$

We also make use of the symmetry condition

$$u_{,x}(-L, z) = u_{,x}(L, z).$$

Physically this means that the incremental strains $\epsilon_x(z)$ are the same on both ends of the beam. With the above conditions, eqn (12) transform as

$$\begin{aligned} A_2\bar{u}_{,zz} - A_1\xi^2\bar{u} + A_3 i\xi\bar{w}_{,z} &= -A_1 i\xi\frac{\Theta}{L}\left(z - \frac{h}{2}\right)\cos n\pi \\ A_4\bar{w}_{,zz} - A_5\xi^2\bar{w} + A_3 i\xi\bar{u}_{,z} &= (A_5 - A_3)\frac{\Theta}{L}\cos n\pi \end{aligned} \tag{16}$$

where

$$\xi = n\pi/L.$$

The solution of the above system of ordinary differential equations consists of complementary functions involving four arbitrary constants and particular integrals as given below.

$$\begin{aligned} \bar{w}(n, z) &= \sum_{i=1}^{4} b_i e^{\rho_i \xi z} - \frac{\Theta}{L\xi^2} \cos n\pi \\ \bar{u}(n, z) &= \sum_{i=1}^{4} d_i e^{\rho_i \xi z} + \frac{i\Theta}{L\xi}\left(z - \frac{h}{2}\right) \cos n\pi \end{aligned} \tag{17}$$

where ρ_is are the roots of the characteristic equation

$$\begin{vmatrix} (A_2\rho^2 - A_1) & A_3 i\rho \\ A_3 i\rho & (A_4\rho^2 - A_5) \end{vmatrix} = 0,$$

b_is are arbitrary constants, and the constants d_i are related to b_i by

$$d_i = \frac{A_3 i\rho_i}{(A_1 - A_2\rho_i^2)} b_i.$$

To evaluate the constants b_i we make use of the boundary conditions (13). The boundary conditions are first expressed in terms of displacements by using the incremental stress-strain relations (10) and strain-displacement relations (9). Then by taking transforms and substituting for $\bar{u}$ and $\bar{w}$ from eqn (17), we obtain the following simultaneous equations in b_is:

$$\sum_{i=1}^{4} \rho_i \left(A_4 - \frac{A_3 B_{31}}{A_1 - A_2\rho_i^2}\right) b_i = -\frac{\bar{p}_1}{\xi}$$

$$\sum_{i=1}^{4} \rho_i e^{\rho_i \xi h} \left(A_4 - \frac{A_3 B_{31}}{A_1 - A_2\rho_i^2}\right) b_i = 0$$

$$\sum_{i=1}^{4} \frac{A_1 + (A_3 - A_2)\rho_i^2}{A_1 - A_2\rho_i^2} b_i = 0$$

$$\sum_{i=1}^{4} e^{\rho_i \xi h} \frac{A_1 + (A_3 - A_2)\rho_i^2}{A_1 - A_2\rho_i^2} b_i = 0.$$

The above equations are solved for b_is and substituted back in eqn (17) to determine $\bar{w}(n, z)$. By taking the inverse transform we obtain

$$w(x, z) = w_0(z) + \sum_{\substack{n=-\infty \\ n\neq 0}}^{+\infty} \bar{w}(n, z) e^{in\pi x/L}.$$

It can be shown that $\bar{w}(n, z) = \bar{w}(-n, z)$ and the solution reduces to

$$w(x, z) = w_0(z) + 2\sum_{n=1}^{\infty} \bar{w}(n, z) \cos n\pi x/L. \tag{18}$$

To evaluate the term $w_0(z)$, we make use of the boundary condition $w(L, z) = 0$. Equation (18) gives the displacements due to load $p_1(x)$. The final solution is the sum of the deflection due to U.D.L. given by eqn (7) and that given by eqn (18).

3. INDENTATION BY A RIGID CYLINDER

The methods developed in Section 2 are used to solve the problem of indentation in an indirect way. We assume that the contact length $2c$ is known and then calculate the contact stresses. Once the stress distribution under the indenter is known, other quantities such as total load, overall deflection of the beam and amount of indentation can be easily computed using the methods described in Section 2. We define the amount of indentation as the difference in the vertical displacements of the indenter and the corresponding point on the bottom side of the beam. In the following subsections, two methods for computing the contact stresses are discussed, i.e. method of point matching, and assumed stress distribution method.

3.1. *Method of point matching*

In this method, contact length $2c$ is assumed to be known *a priori*. Also, the contact stress distribution is discretized and considered to be the superposition of a finite number of symmetrical rectangular loadings of unknown magnitudes distributed over known lengths (Figure 2b). For example, the contact length $2c$ may be divided into m equal parts. Thus, the jth load distribution is of magnitude q_j and its span is $2cj/m$. The m number of equations required to solve for the unknown qs are set up by the fact that the indented surface lies on a circular arc of radius R which is also the radius of the indenter. To achieve this we consider m reference points on the contact surface excluding the center point. We define the following notations: w_{jk} is the vertical displacement of jth reference point due to kth load distribution of unit magnitude; w_{0k} is the vertical displacement of the mid-point of contact area due to kth load distribution of unit magnitude; w_j is the vertical displacement of jth point due to indentation; w_0 is the vertical displacement of mid-point due to indentation; and x_j is the x-coordinate of jth reference point.

For small contact lengths we can use the following approximate relation

$$(w_0 - w_j) \simeq x_j^2/2R. \tag{19}$$

But from the definitions

$$w_0 = \sum_{k=1}^{m} w_{0k} q_k \tag{20}$$

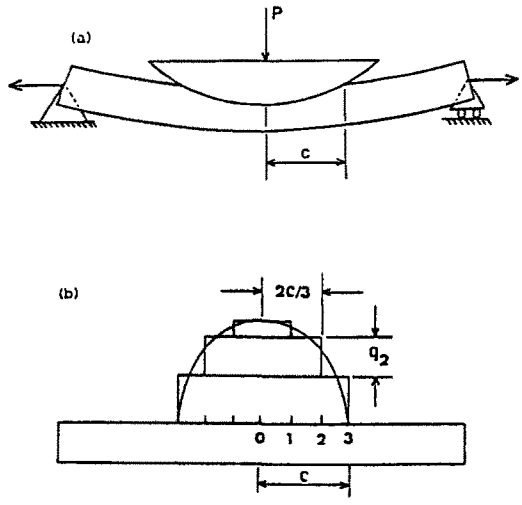

Fig. 2. (a) Cylinder indenting a beam under initial stresses. (b) Discretization of contact stress distribution.

and

$$w_j = \sum_{k=1}^{m} w_{jk} q_k. \tag{21}$$

From eqns (19–21) we obtain

$$\sum_{k=1}^{m} (w_{0k} - w_{jk}) q_k = x_j^2/2R, \quad j = 1, \ldots, m. \tag{22}$$

The quantities w_{0k} and w_{jk} are displacements due to unit stress distributions over known spans and they may be computed using methods discussed in Section 2. The m simultaneous equations (22) may be solved for the m unknown qs. From the contact stress distribution other quantities of interest such as total load, vertical displacements and the amount of indentation may be computed. By varying the contact length $2c$, a whole series of load-indentation relations may be developed.

The optimum number of divisions m depends upon the contact length and also the stress gradients. For example, in the beginning of indentation, contact stress distribution is nearly elliptical. So, even a small number of divisions yield converging results. As the contact length increases, there is a peaking of stresses at the ends of the contact zone and it requires larger number of divisions to get more accurate results. In the numerical examples m was varied from 10–40 depending on the contact length. The results obtained using the point matching technique are presented in Section 4.1.

3.2. *Method of assumed stress distribution*

As will be discussed later, for small contact lengths (e.g. $c/h \leq 0.5$) the contact stress distribution may be represented by an ellipse; i.e. the stresses under the indenter are given by

$$p(x) = p_0(1 - x^2/c^2)^{1/2}. \tag{23}$$

In the above equation c is the semi contact length and p_0 is the maximum value of the stress at the center. As before, we start with a known contact length $2c$ leaving p_0 as an unknown. Then we assume a similar stress distribution with some arbitrary p_0, say p_0', and compute the vertical displacements of the points in the contact zone. The average radius of curvature of the indented surface R' may be calculated using the relation

$$R' = \frac{1}{m} \sum_{j=1}^{m} \frac{x_j^2}{2(w_0 - w_j)}$$

where m is the number of reference points over the contact length; x_j is the x-coordinate of jth reference point; w_0 is the vertical displacement of the center point; and w_j is the vertical displacement of the jth point. Generally, R' will be different from the radius of the indenter R. But, the displacements vary linearly with the load and hence the peak stress p_0 required to produce a radius R is given by

$$p_0 R = p_0' R'$$

The desired load distribution is then given by eqn (23). The vertical displacements and indentation may be calculated using the methods explained earlier.

4. RESULTS AND DISCUSSIONS

The numerical results presented in this section were obtained by using the assumed stress distribution method for $c/h \leq 0.2$ and the point matching technique for $c/h \geq$

Table 1. Properties of the orthotropic materials used in the numerical examples

Material Property	1	2	3
E_1(GPa)	34.5	34.5	34.5
E_3/E_1	0.9	0.067	15.0
G_{13}/E_1	0.35	0.026	0.38
ν_{13}	0.3	0.3	0.02
ν_{31}	0.27	0.02	0.3

0.1. In all the examples, E_1, the Young's modulus in x-direction is kept as a constant equal to 34.5 GPa(5×10^6 psi). The length of the beam is assumed as 50.8 mm (2 inches), and thickness is 2.54 mm (0.1 in.). The width in the y-direction is taken as 25.4 mm (1 inch) and radius of the indenter is assumed to be 25.4 mm (1 inch).

As mentioned earlier, our discussions focus on (i) the effect of orthotropy and (ii) the effect of initial stresses on the contact behavior. To study the effect of orthotropy, we consider three different material systems. Their properties are presented in Table 1. In Table 1, G_{13} is the transverse shear modulus, ν_{13} and ν_{31} are the Poisson's ratios when loads are applied in the x and z directions, respectively.

Material 1 is nearly isotropic and it is considered in the present study so that the results can be compared with those for an isotropic beam presented in [3]. Materials 2 and 3 have E_3, the transverse Young's modulus, quite different from E_1. The effect of initial stresses is studied with beam made of Material 1. Both tensile and compressive initial stresses are considered. The value of tensile stress considered in the example is equal to 0.02 E_1. The compressive stress is 0.001 E_1, which corresponds to about half the buckling load for the beam considered.

4.1. *Effect of orthotropy on contact behavior*

Curves in Figs. 3–10 depict the contact behavior of the three orthotropic beams. Initial stresses are not considered in these examples.

4.1.1. *Contact stresses.* The nondimensional contact stress distribution $p(x)$ for beam 1 is shown in Fig. 3. The stress distribution is plotted for various values of c/h.

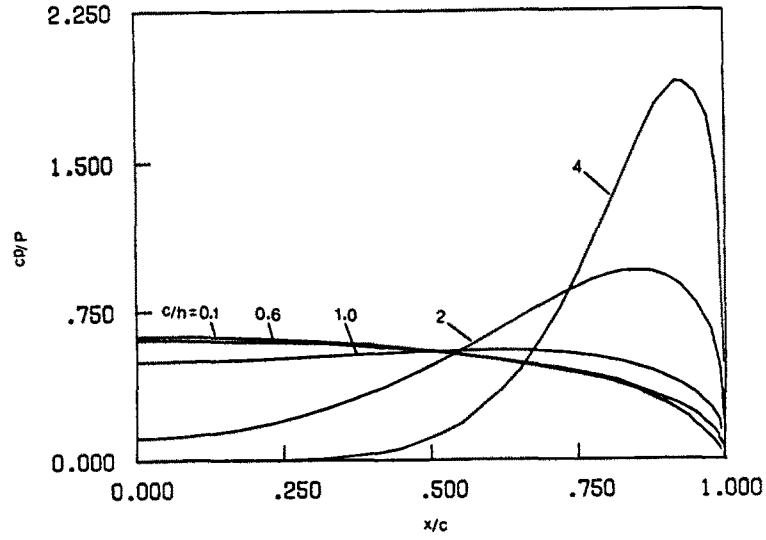

Fig. 3. Contact stresses in beam 1 (E_3/E_1 = 0.9, p: contact stress, P: total load).

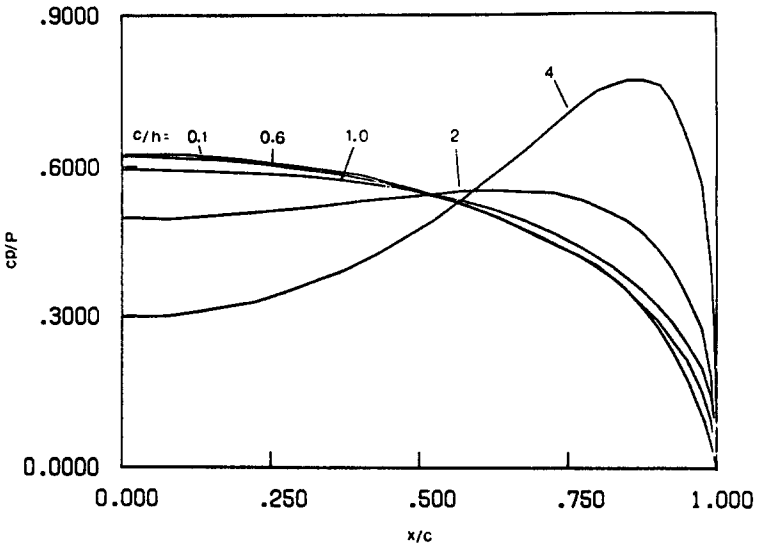

Fig. 4. Contact stresses in beam 2 (E_3/E_1 = 1/15).

Actually the discretized stress distributions obtained through the use of point matching technique are smoothed out in the figures. From Fig. 3 it can be seen that the nondimensionalized contact stresses are close to the results of the isotropic beam given in [3]. For small contact lengths ($c/h \leq 0.6$) the contact stress distribution is nearly elliptical. On further indentation, the stresses in the central portion of the contact zone decreases whereas there is peaking of stresses at the ends. As the beam wraps around the indenter (e.g. $c/h = 4$), the contact stresses in the central portion becomes zero. This behavior has been the discussion of [1] and [3].

From Fig. 4 it may be seen that a reduction in Young's modulus E_3 does not affect the nature of contact stress distribution at the beginning of indentation. Even for large c/h values, the deviation from the elliptical distribution is less when compared to beam 1. But opposite is the case when E_3 is increased. Figure 5 shows that in beam 3 ($E_3/E_1 = 15$) deviation from the elliptical stress distribution starts earlier and also, the peaking of stresses is more severe. The conclusion is that the local indentation behavior very much depends on E_3 whereas E_1 controls the wrapping behavior and is responsible for the peaking behavior discussed earlier.

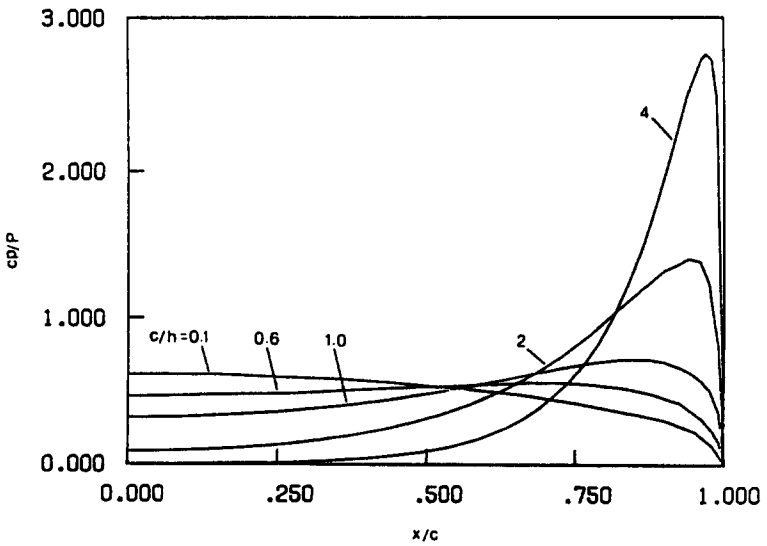

Fig. 5. Contact stresses in beam 3 (E_3/E_1 = 15).

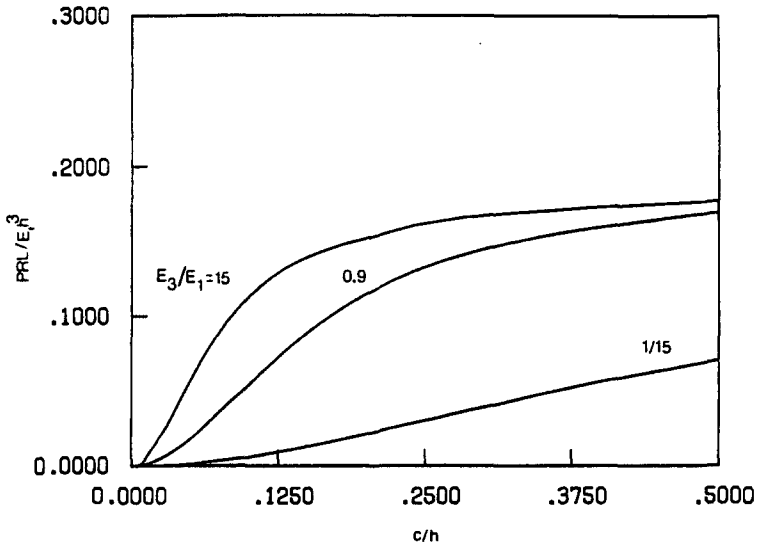

Fig. 6. Load-contact length relation (no initial stresses).

4.1.2. *Load-contact length relation.* The load-contact length relationship is depicted in Fig. 6. As can be seen, the load required to produce a given contact length depends on the value of E_3. However, at higher loads wrapping behavior dominates the indentation behavior. The increase in contact length is essentially due to beam bending rather than indentation. Moreover, it may be seen that in beams 1 and 3, there is a rapid increase in contact length even for small load increments, when the nondimensional load is about 0.167. This is the point where the average radius of curvature of the beam at the center approaches that of the indenter. In the case of beam 2, this effect is not as significant and also it occurs at a lower load. The reasons are lower value of E_3 and also lower G_{13} (see Table 1).

4.1.3. *Overall beam stiffness.* Curves in Figure 7 depict the relation between total load and the center point deflection which is also the displacement of the indenter. The relations are linear until wrapping begins. At higher loads, the beam apparently becomes stiffer. Though E_1 is the same for all beams, beam 2 is less stiff than the other two because of lower shear modulus G_{13}.

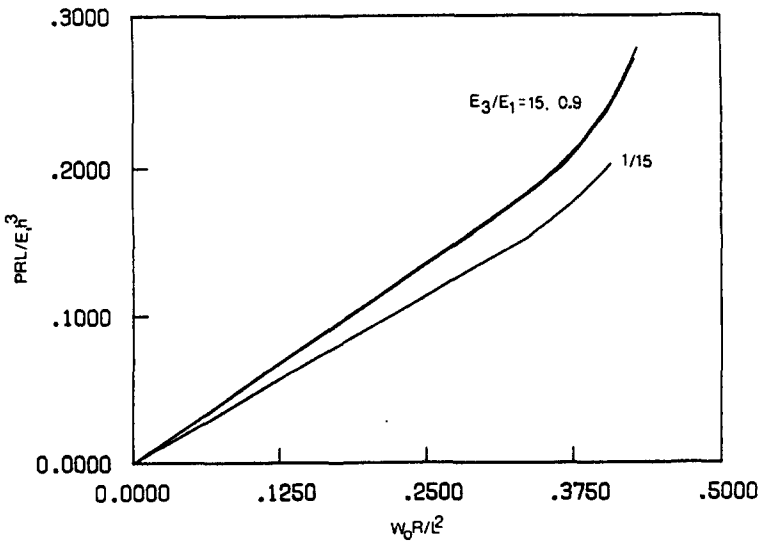

Fig. 7. Load versus indenter displacement (no initial stresses).

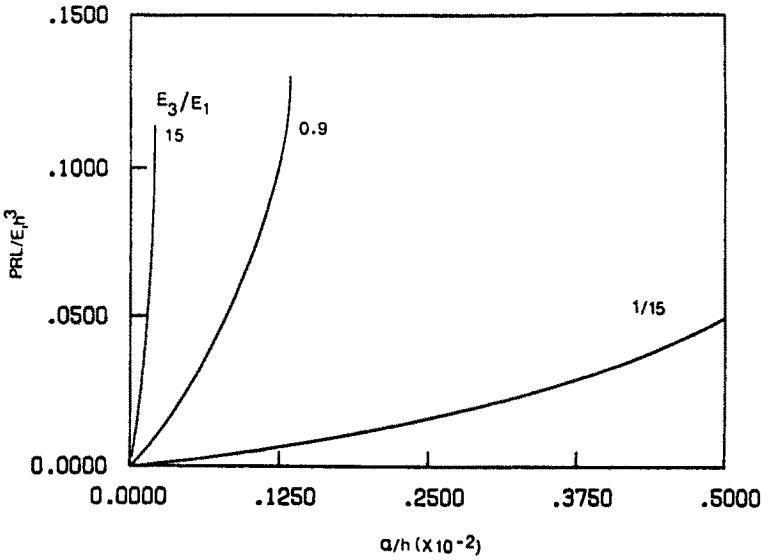

Fig. 8. Load-indentation relation (no initial stresses, α: indentation).

4.1.4. *Indentation law.* As can be seen from Fig. 8, the amount of indentation increases with the load up to a certain point and then starts decreasing with increasing load. This is due to the distribution of load over larger contact area at higher loads. It may be noted that the initial portion of the load-indentation relation, where the bending is not much in effect, may be approximated by a power law of the type

$$P^* = k^* \alpha^{*q}$$

where

$$P^* = PRL/E_1 h^3$$

$$\alpha^* = \alpha/h$$

q = exponent of the indentation law

k^* = dimensionless contact coefficient.

Least squares fitting of the data shown in Fig. 8 gives an average value of $q = 1.18$. The values of k^* are tabulated in Table 2. From this table it is obvious that the transverse Young's modulus E_3 has more effect on k^*. In general, k^* is a function of the elastic constants of the beam material and radius of the indenter. The exact functional form has not yet been found out.

4.2. *Effect of initial stresses on contact behavior*

Beam 1 which is nearly isotropic is considered in the study of the effect of initial stresses on contact behavior. The idea is to distinguish between the initial stress effect and that due to orthotropy. Both tensile and compressive initial stresses along the x-direction are considered.

Table 2. Indentation law constants for the three orthotropic materials

	Beam 1	Beam 2	Beam 3
E_3/E_1	0.9	1/15	15
k^*	215.4	17.24	1634

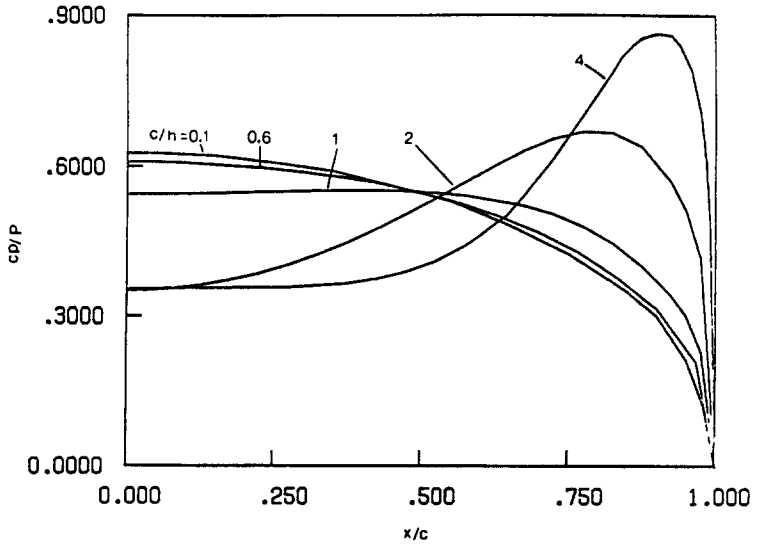

Fig. 9. Contact stresses in beam 1 under initial tension ($S_0 = +0.02E_1$).

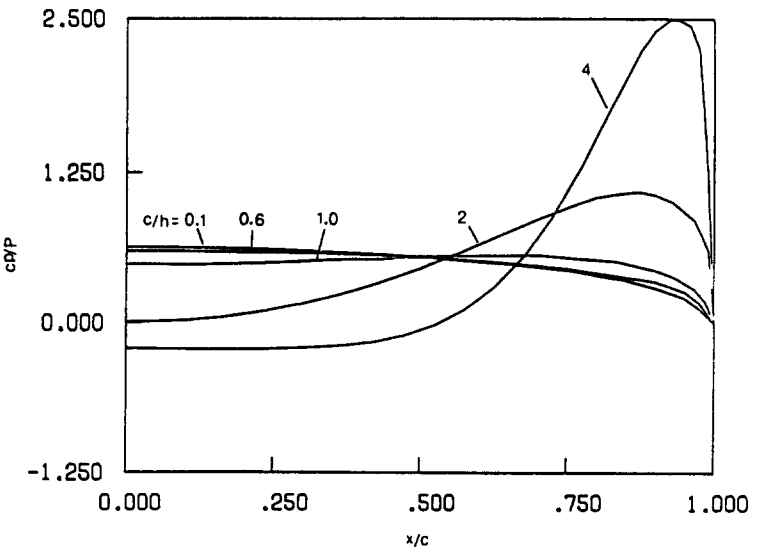

Fig. 10. Contact stresses in beam 1 under initial compression ($S_0 = -0.001E_1$).

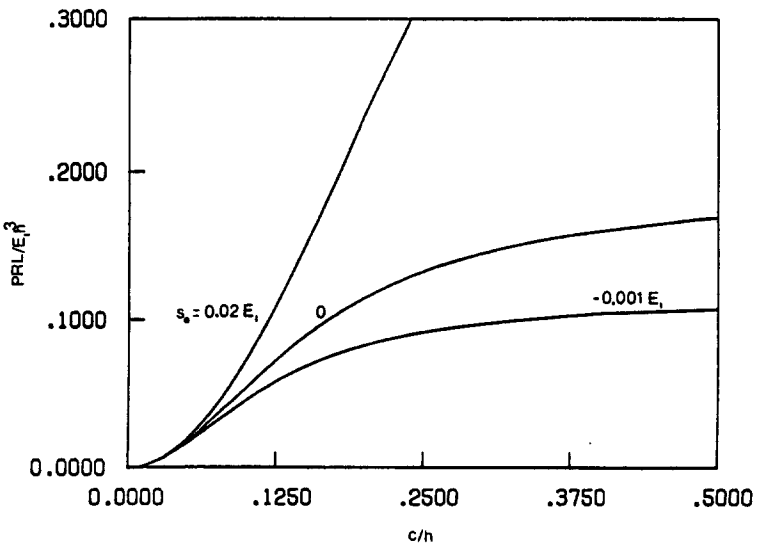

Fig. 11. Load-contact length relation for beam 1 under initial stresses.

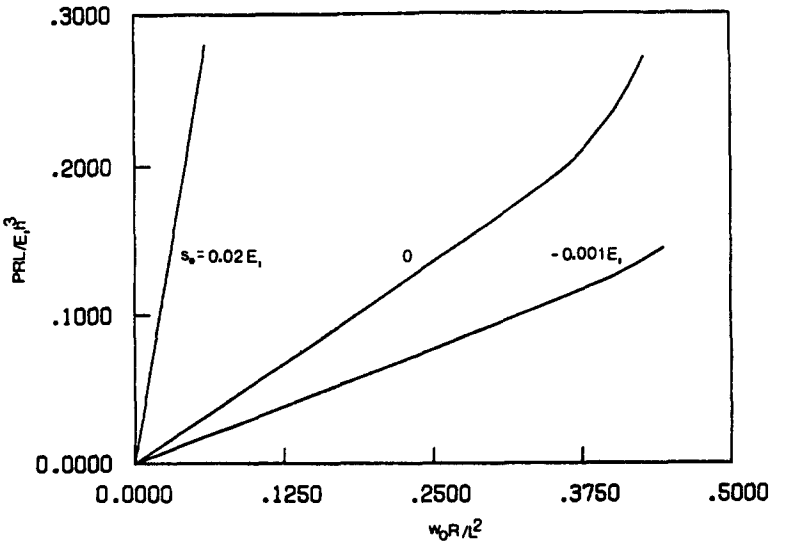

Fig. 12. Load versus indenter displacement for beam 1 under initial stresses.

4.2.1. *Contact stresses.* Figure 9 shows the stresses under the indenter for various c/h values when the beam is under initial tension. Again, for small c/h values the stress distribution is elliptical. But for higher c/h (e.g. $c/h = 4$), the stresses in the central portion of the contact area do not become zero (*cf* Fig. 3), but remain at a constant value. This contact stress is necessary to equilibrate the vertical component of the initial stresses in the bent beam. In fact, this constant value of stress is found to be nearly equal to N_x^0/R, where N_x^0 is the initial stress resultant and R is the radius of the indenter.

Curves in Fig. 10 depict the contact stress distribution when the initial stresses are compressive. At the beginning of indentation, as expected, the contact stress distribution is elliptical. But at higher contact lengths (e.g. $c/h = 4$), the contact stresses at the center become negative, implying tensile stresses. As in reality such negative contact stresses cannot exist, this suggests possible loss of contact and redistribution of contact stresses. The present analysis is not valid beyond this point and we may have to resort to a trial and error method for an exact analysis.

4.2.2. *Load-contact length relations.* Figure 11 shows the load-contact length relationship for various values of initial stresses. At the beginning of indentation, when

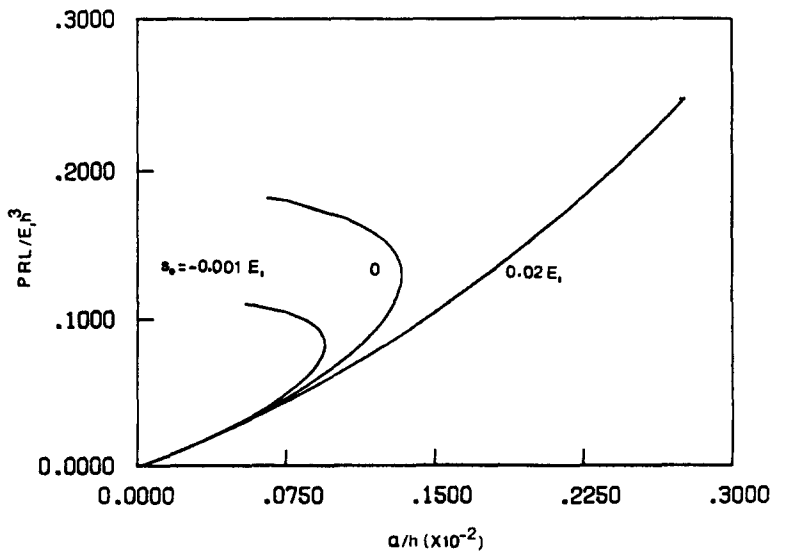

Fig. 13. Load-indentation relations for beam 1 under initial stresses.

bending has not come into effect, all the three curves are indistinguishable, indicating that the initial stresses have no significant effect on the contact behavior. In fact, the initial stresses do not affect the contact behavior directly, but they modify the flexural rigidity of the beam which in turn affects the contact behavior. This is evident from Fig. 11 where one can see that wrapping of the beam around the indenter begins at different values of the total load.

4.2.3. *Overall beam stiffness.* Figure 12 shows the effect of initial stresses on the flexural rigidity of the beam. The results reveal no surprises.

4.2.4. *Load-indentation relations.* The load-indentation relations shown in Fig. 13 reiterate the fact that the presence of initial stresses is not felt appreciably until the bending effects come into picture. For small contact lengths, the indentation law remains unchanged irrespective of the initial stresses. Deviation from this law occurs earlier when the initial stresses are compressive. With tensile initial stresses, the same indentation law may be considered to be valid even for slightly higher loads. It is interesting to note that the presence of tensile initial stresses makes indentation easier while compressive initial stresses make indentation harder.

Acknowledgment—This work was supported by a NASA-Langley Research Center Grant No. NAG 1222 with Purdue University.

REFERENCES

1. L. M. Keer and G. R. Miller, Smooth indentation of a finite layer, *J. Engng Mech. Div. ASCE* **109**, 706 (1983).
2. L. M. Keer and R. Ballarini, Smooth contact between a rigid indenter and an initially stressed orthotropic beam, *AIAA J.* **21**, 1035 (1983).
3. B. V. Sankar and C. T. Sun, Indentation of a beam by a rigid cylinder, *Int. J. Solids Structures* **19**, 293 (1983).
4. M. A. Biot, *Mechanics of Incremental Deformations*. Wiley, New York, (1965).
5. C. T. Sun and S. Chattopadhyay, Dynamic response of anisotropic laminated plates under initial stresses to impact of a mass, *J. Appl. Mech. ASME* **42**, 683 (1975).
6. J. M. Whitney and N. J. Pagano, Shear deformation in heterogeneous anisotropic plates, *J. Appl. Mech. ASME* **37**, 1031 (1970).